Proceedings of ISAP'04, Sendai, JAPAN

DESIGN METHOD OF NARROW-WIDTH FERMI ANTENNA FOR PASSIVE MILLIMETER WAVE IMAGING

Hiroyasu SATO, Syunichi KAGAYA†, Yoshihiko WAGATSUMA†,
Kunio SAWAYA, and Koji MIZUNO†
Graduate School of Engineering, Tohoku University
Aza-Aoba 05, Aramaki, Aobaku, Sendai, 980-8579, Japan
† Research Institute of Electrical Communication, Tohoku University
2-1-1, Katahira, Aobaku, Sendai, 980-8577, Japan
E-mail: sahiro@sawaya.ecei.tohoku.ac.jp

1. INTRODUCTION

Development of a receiving element suitable for passive millimeter-wave (PMMW) imaging array is desired [1], [2]. Required characteristics of the antenna for the array are: the same E-plane and H-plane patterns (circular radiation pattern) having desired beam width to achieve the optimum coupling with a dielectric lens, a narrow-width geometry to obtain a high resolution of imaging and broad bandwidth.

The tapered slot antenna (TSA) is well known for the features of thin structure, low weight, easy to fabricate, broadband and well suited for microwave integrated circuits (MICs), and is expected to meet a demands described above.

Recently, *Sugawara et al.* have proposed a TSA called "FERMI antenna" [3], [4] having a profile defined by the Fermi-Dirac function as well as the corrugation on the side of the substrate. They found experimentally that the FERMI antenna has almost the same E-plane and H-plane patterns and low side lobe levels.

However, the TSA's including the FERMI antenna have many design parameters such as the taper profile, the length of antenna, the width of aperture, the thickness and dielectric constant of the substrate, the dimensions of the ground plane, and these parameters affect the radiation characteristics.

The purpose of this paper is to develop a design method using the FDTD to obtain the parameters of the FERMI antenna for PMMW imaging, and to show an optimum design.

2. GEOMETRY

Fig. 1 shows the geometry of the FERMI antenna. The Fermi-Dirac taper is determined

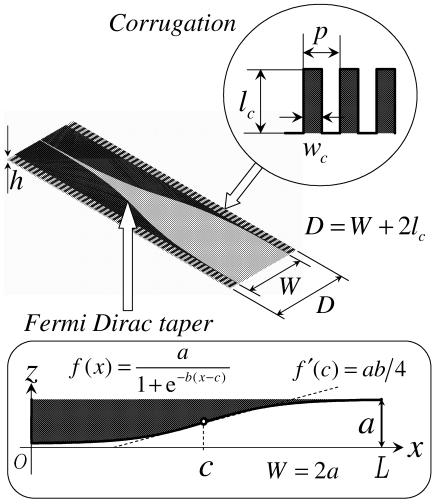

Figure 1: Geometry of FERMI antenna.

by the following equation

$$f(x) = \frac{a}{1 + e^{-b(x-c)}} \tag{1}$$

where a denotes the asymptotic value of the width of the taper for $x \to \infty$ and c denotes the x coordinate of the inflection point of the Fermi-Dirac function. Because of the relation of $f'(c) = ab/4$, b is related to the gradient at the inflection point c. Also there is a relation of $f(c) = a/2$ and $W = 2a$ when $b(L - c) \gg 1$.

The FDTD analysis was performed to find the relation between the radiation pattern and the parameters of the FERMI antenna fabricated on a 200μm-thick dielectric substrate (ε_r=3.7). The length of antenna L is selected as $4\lambda_0$ so that the taper section holds traveling wave characteristics [3], where λ_0 is the wavelength in vacuum at the center frequency. The width of the aperture W and the position of the inflection point c is optimized in Sec. 3 to

ISBN: 4-88552-207-2 C3055©IEICE

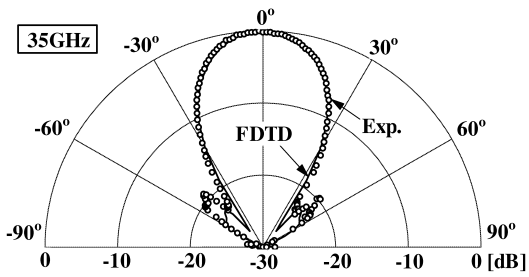

(a) E-plane

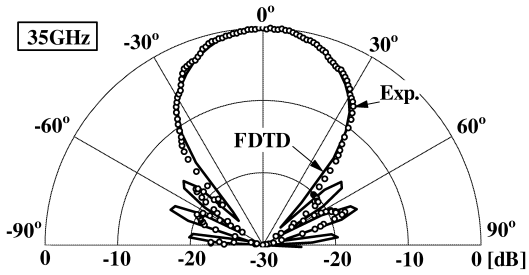

(b) H-plane

Figure 2: Radiation pattern of FERMI antenna at 35 GHz. W=0.91λ_0, a=$W/2$, b=2.4/λ_0, c=2λ_0.

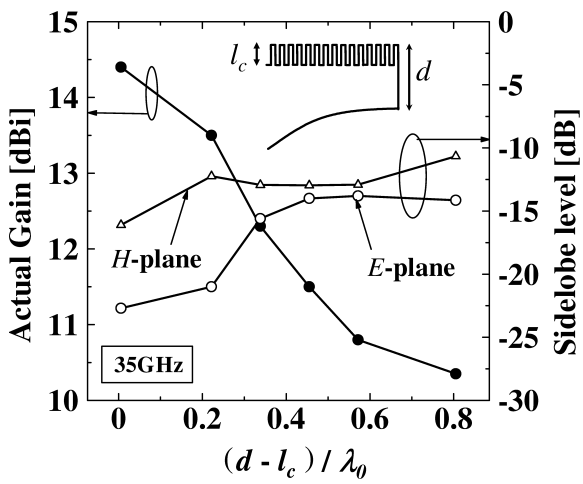

Figure 3: Calculated actual gain and sidelobe levels of FERMI antenna with changing d while l_c=0.13λ_0, W=0.91λ_0, a=$W/2$, b=2.4/λ_0, c=2λ_0.

obtain a narrow-width FERMI antenna with the required circular radiation pattern. The dimensions of the corrugation with the width w_c, the pich p and the length l_c are determined as [4],

$$w_c = L/100, \quad p = 2w_c, \quad l_c = 0.13\lambda_0 \quad (2)$$

and the parameter b is selected as 2.4/λ_0 [5] to obtain low side lobe level of the H-plane pattern.

3. DESIGN FOR PMMW IMAGING

The FDTD numerical design of the radiation pattern to obtain the 10dB beam width of BW$_{design}$=52° which is suitable for our f/D=1 focusing system [6], was performed. In the FDTD analysis, the cell size are Δx=0.1714mm, Δy=0.1mm and Δz=0.05mm, respectively. The number of time steps was 16,000 and the 8-layer PML was used. The antenna was separated 40Δx, 20Δy and 60Δz from the PML in each direction. A gaussian pulse was used for the excitation of the antenna at the origin O in Fig. 1 and the delta gap feed was used with 110 Ω internal resistance, which is corresponding to the characteristic impedance of the feeding slot line with the width of 0.1mm.

Fig. 2 (a), (b) compare the radiation patterns of a typical Fermi antenna measured and calculated at 35GHz which is an atmospheric window. The width of the aperture W and the position of the inflection point c were selected as W=0.91λ_0 and c=2λ_0, respectively, where λ_0 is the wavelength at f_0=35GHz. In the experiments, the feeding slot line was excited by a waveguide-to-finline transition, and the finline was inserted inside the rectangular waveguide WRJ-320. Good agreement between the numerical results and the experimental data is observed and the validity of FDTD analysis is confirmed.

Fig. 3 shows the calculated actual gain and sidelobe levels of the FERMI antenna as a function of the width of the lateral edge d. It is observed that the gain increases and the sidelobe levels of the E-plane and the H-plane decrease for narrower d, *i.e*, $d = l_c$. Thus, the width of the substrate D should be selected as $D = W + 2l_c$ to obtain a narrow-width FERMI antenna with high gain and low sidelobe levels.

Fig. 4 (a) shows the 10dB beam width of the radiation pattern as a function of the position of the inflection point c when the width of the aperture is W=0.91λ_0. The beam width of the H-plane changes from 70.4^o to desired beam width BW$_{design}$=52° when c moves from 2λ_0 to λ_0, while the variation of beam width of the E-plane is 7.5^o. When c equals to λ_0, the beam

width of the E-plane is 45°, resulting in almost circular radiation pattern. Simulated results of the 10dB beam width versus the width of the aperture W ($0.3\lambda_0$–$0.9\lambda_0$) are shown in Fig. 4 (b), when c=λ_0. The beam width of the E-plane changes from 45° to BW_{design}=52° while the variation of the beam width of the H-plane is only 1°.

Thus, the beam width of the E-plane is almost determined by the width of the aperture W and that of the H-plane is determined by the position of the inflection point c. It has been found that a narrow-width FERMI antenna having beam widths of nearly 52° in both E-plane and H-plane can be obtained by selecting c=λ_0 and W=$0.32\lambda_0$.

Fig. 5 show the optimized radiation patterns of a FERMI antenna measured and calculated at 35GHz. The circular radiation pattern is obtained with low sidelobe levels in the E-plane and the H-plane for the narrow-width FERMI antenna. The width of the substrate D=5mm is almost equal to the half Rayleigh resolution of 5.25mm at 35GHz.

Fig. 6 shows the calculated frequency characteristics of 10dB beam width. It is observed that almost the same E-plane and H-plane beam widths are obtained in the broadband frequency range which is required in PMMW imaging.

In order to evaluate the optical matching between the lens and the FRRMI antenna, the coupling factor [7], [8] with respect to the electric field given by

$$\alpha = \frac{|\int_{-\frac{\pi}{2}}^{\frac{\pi}{2}} q(\theta) f^*(\theta) d\theta|^2}{\int_{-\frac{\pi}{2}}^{\frac{\pi}{2}} |q(\theta)|^2 d\theta \int_{-\frac{\pi}{2}}^{\frac{\pi}{2}} |f(\theta)|^2 d\theta} \qquad (3)$$

was introduced, where $f(\theta)$ is the radiation pattern of the FERMI antenna and $q(\theta)$ is the field distribution of the lens given by

$$q(\theta) = \begin{cases} 1, & |\theta| < 26^\circ \\ 0, & \text{else.} \end{cases} \qquad (4)$$

The calculated results in the case of Fig. 2 (unoptimized) and Fig. 5 (optimized) were 75% and 81%, respectively, resulting in the increase of the transformation efficiency.

4. CONCLUSION

A design of the FERMI antenna as a receiving element of PMMW imaging has been presented. By using the FDTD analysis, it has been found that the beam width of the E-plane and the H-plane of the FERMI antenna can be controlled by changing the width of the aperture and the position of the inflection point of the Fermi-Dirac taper profile, respectively. According to these characteristics, a FERMI antenna with the circular radiation pattern having the beam width of 52° and the geometrical width of $0.58\lambda_0$ which fits to the f/D=1 optics have been obtained.

REFERENCES

[1] K. Uehara, K. Miyashita, K. Natsume, K. Hatakeyama and K. Mizuno, "Lens-coupled imaging arrays for the millimeter- and submillimeter-wave regions," IEEE Trans. Microwave Theory Tech., vol. 40, no. 5, pp. 806–811, May 1992.

[2] K. Mizuno, "Millimeter wave imaging technologies (Invited)," in Proc. 2001 Asia-Pacific Microwave Conference, pp. 394-398, Taipei, Dec. 2001.

[3] S. Sugawara, Y. Maita, K. Adachi, K. Mori and K. Mizuno, "A mm-wave tapered slot antenna with improved radiation pattern," IEEE MTT-S International Microwave Symposium Digest, pp. 959–962, Denver, USA, 1997.

[4] S. Sugawara, Y. Maita, K. Adachi, K. Mori and K. Mizuno, "Characteristics of a mm-wave tapered slot antenna with corrugated edges," IEEE MTT-S International Microwave Symposium Digest, pp. 533–536, Baltimore, USA, 1998.

[5] H. Sato, N. Arai, Y. Wagatsuma, K. Sawaya and K. Mizuno, "Design of Millimeter Wave Fermi Antenna with Corrugation," IEICE Trans. (B), vol. J86-B, no. 9, pp. 1851–1859, 2003 (in Japanese).

[6] A. R. Gillespie and T. G. Phillips, "Array Detectors for Millimetre Line Astronomy," Astron. Astrophys. vol. 73, pp. 14–18, 1979.

[7] K. Mizuno, T. Suzuki, S. Ono, and K. Sagae, "Optimum coupling of a gaussian beam to a corner reflector with a four-wavelength antenna," Int. J. Infrared and Millimeter Waves, vol. 4, no. 3, pp. 321-325, 1983.

[8] S. E. Schwarz, "Efficiency of Quasioptical Couplers," Int. J. Infrared and Millimeter Waves, vol. 5, pp. 1517-1525, 1984.

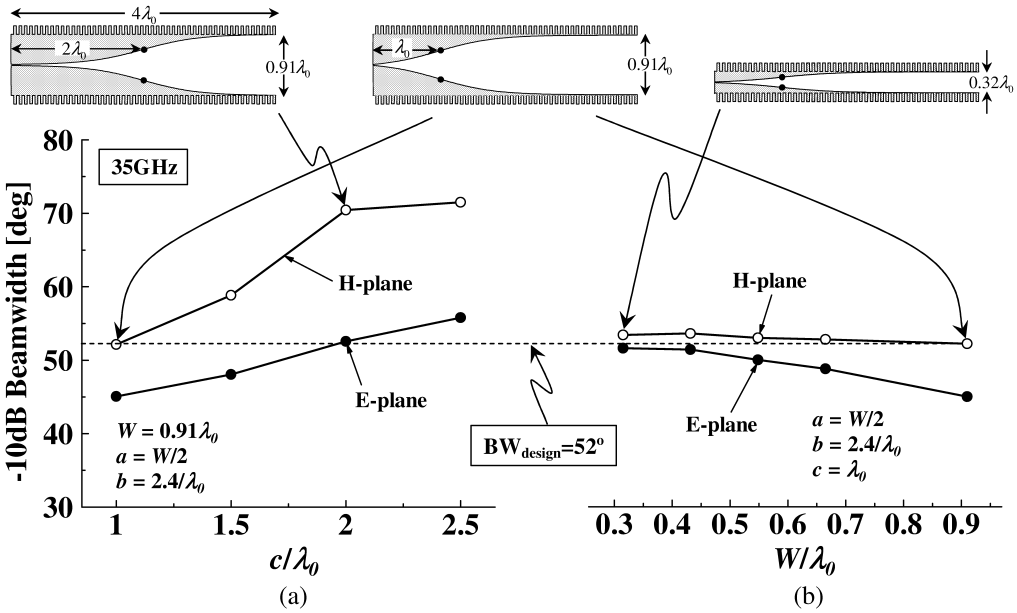

Figure 4: 10dB beam width of FERMI antenna, (a) as a function of position of inflection point c (W=0.91λ_0), (b) as a function of width of aperture W (c=λ_0).

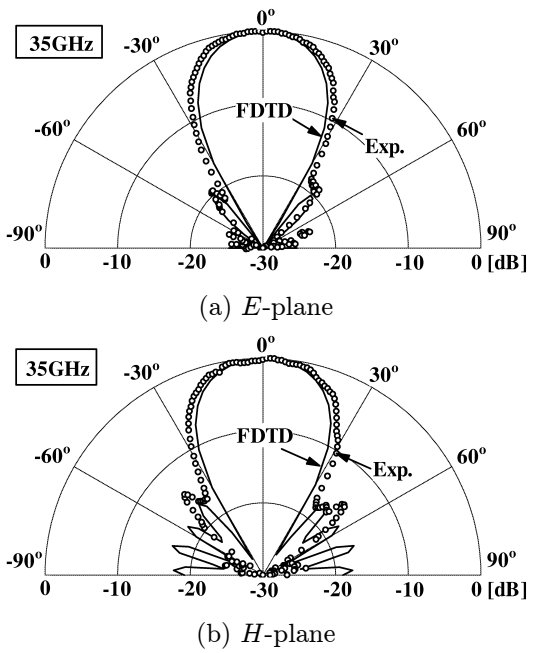

(a) E-plane

(b) H-plane

Figure 5: Optimized radiation pattern of FERMI antenna at 35 GHz, W=0.32λ_0, a=$W/2$, b=2.4/λ_0, c=λ_0.

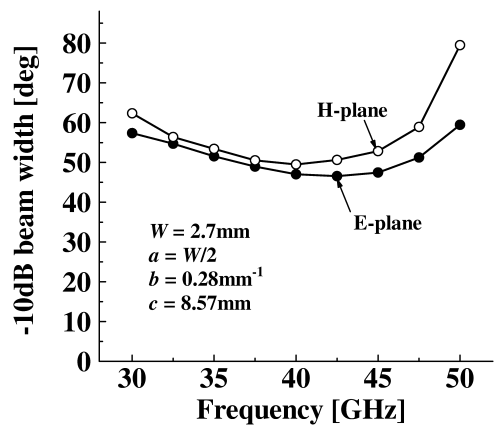

Figure 6: Calculated 10dB beam width of FERMI antenna as a function of frequency.